

# Episodic accretion onto a protostar

Tomoyuki Hanawa<sup>1</sup>, Nami Sakai<sup>2</sup> and Satoshi Yamamoto<sup>3</sup>

<sup>1</sup>Center for Frontier Science, Chiba University, 1-33 Yayoi-cho, Inage-ku, Chiba 263-8522, Japan

email: [hanawa@faculty.chiba-u.jp](mailto:hanawa@faculty.chiba-u.jp)

<sup>2</sup>RIKEN Cluster for Pioneering Research, 2-1 Hirosawa, Wako-shi, Saitama 351-0198, Japan

email: [nami.sakai@riken.jp](mailto:nami.sakai@riken.jp)

<sup>3</sup> Department of Physics, The University of Tokyo, Bunkyo-ku, Tokyo 113-0033, Japan

email: [yamamoto@taurus.phys.s.u-tokyo.ac.jp](mailto:yamamoto@taurus.phys.s.u-tokyo.ac.jp)

**Abstract.** We introduce hydrodynamic simulations in which a protostar captures a cloudlet with a relatively small angular momentum. The cloudlet accretes onto the protostar and perturbs the gas disk rotating around the protostar. This cloudlet capture can reproduce some features observed in the molecular emission lines from TMC-1A. First, the cloudlet can reproduce the blue asymmetry observed in the CS emission. Second, the cloudlet can explain the slow infall observed in the C<sup>18</sup>O emission. Third, the impact of the cloudlet can explain the offset of the SO emission from the disk center. We also argue that a warm gas should confine the cloudlet through pressure. A protostar may obtain substantial mass by capturing cloudlets.

**Keywords.** Young stellar objects – Interstellar medium – Interstellar molecules – Protostars – Star formation

---

## 1. Introduction

Gas accretion is one of the important characteristics of young stellar objects. It supplies mass and angular momentum to the disks rotating around the central stars. Though the accretion rate tends to decline with age, it is variable and may be sporadic. We often assume that the gas accretion is more or less symmetric unless the system does not contain binary or multiple stars. However, some protostars show a highly asymmetric Doppler shift in the molecular emission lines observed with ALMA (see, e.g., [Yen et al. 2014](#) for L1489 IRS; [Sakai et al. 2016](#) for TMC-1A). More recently [Garufi et al. \(2022\)](#) have detected SO and SO<sub>2</sub> emissions in the region of disk impacted by gas streamer in DG Tau and HL Tau. These observations suggest the possibility that the gas accretion is intrinsically asymmetric in these systems.

Gas accretion onto more evolved objects can also be asymmetric. [Dullemond et al. \(2019\)](#) have demonstrated that capture of a cloudlet forms an arc-like feature observed in AB Aur. The cloudlet capture model can explain the misalignment of inner and outer disks observed in some transitional systems ([Küffmiejr et al. 2021](#)). It can also explain variability in the accretion rate because the capture should be episodic.

The cloudlet capture model assumes that the accreting gas has a relatively small angular momentum and hence the centrifugal radius is small. Then, the accreting gas approaches the central star without losing the angular momentum. This mode of gas accretion is quite different from the classical picture in which the angular momentum transfer drives gas accretion. The cloudlet capture is similar to the ballistic model of an infalling–rotating envelope of [Sakai et al. \(2016\)](#) in which the centrifugal radius is

100 au. The ballistic model, however, does not take into account hydrodynamic effects and asymmetry. Here we introduce our hydrodynamic simulations for TMC-1A in which a protostar associated with a rotating gas disk captures a cloudlet. The cloudlet collides with the disk and destroys a part of it. The model can explain the observed asymmetry in the molecular emission lines from TMC-1A.

## 2. Model and Methods

We consider the three components of gas, cloudlet and gas disk, as well as the surrounding warm medium, in our simulations. Both the cloudlet and gas disk consist of cold molecular gas, while the warm gas consists of warm atomic gas. All these components should remain nearly isothermal because the thermal timescale is much shorter than the dynamical timescale. We employ an artificially low specific heat ratio,  $\gamma = 1.05$ , and do not take into account heating and cooling explicitly to mimic the nearly isothermal state. We assume that the mass of the central star is  $M = 0.53 M_{\odot}$ , though it is highly uncertain in the literature. We do not consider the magnetic fields and the self-gravity for simplicity. Hence, the basic equations are expressed as

$$\frac{\partial \rho}{\partial t} + \nabla \cdot (\rho \mathbf{v}) = 0, \quad \frac{\partial}{\partial t}(\rho \mathbf{v}) + \nabla \cdot (\rho \mathbf{v} \mathbf{v} + P) = \rho \mathbf{g}, \quad \mathbf{g} = -\frac{GM}{\max(|\mathbf{r}|, a)^3} \mathbf{r}, \quad (2.1)$$

$$\frac{\partial}{\partial t}(\rho E) + \nabla \cdot [(\rho E + P)\mathbf{v}] = \rho \mathbf{v} \cdot \mathbf{g}, \quad E = \frac{\mathbf{v}^2}{2} + \frac{P}{(\gamma - 1)\rho}, \quad (2.2)$$

where  $\rho$ ,  $P$ ,  $\mathbf{v}$ , and  $G$  denote the density, pressure, velocity, and gravitational constant, respectively. We reduce the gravitational acceleration,  $\mathbf{g}$ , artificially in the region of  $r \leq a = 50$  au to avoid too steep pressure gradient.

We use the cylindrical coordinates,  $(r, \varphi, z)$ , in our hydrodynamic simulations. The central star is located at the origin of the cylindrical coordinates. We integrate the hydrodynamic equations according to Hanawa & Matsumoto (2021) so that we can achieve both the angular momentum conservation and free-stream preservation. Our numerical code does not take account of the increase in the protostar mass. The spatial resolution is  $\Delta r = \Delta z \simeq r \Delta \varphi = 1.0$  au in the region of  $|r| \leq 64$  au and  $|z| \leq 64.5$  au, while it is  $\Delta r/r \simeq \Delta z/|z| \simeq \Delta \varphi = 1/64$ .

The warm gas has mean molecular weight of  $1.27 m_{\text{H}}$ , respectively, at the initial stage, where  $m_{\text{H}}$  denotes the mass of hydrogen atom. The warm gas is in hydrostatic equilibrium. The gas disk has a radius of 100 au and is supported mainly by the centrifugal force against gravity. The gas disk is in hydrostatic balance in the vertical direction with the surrounding warm gas. The cloudlet has the same pressure as the surrounding warm gas and a uniform velocity corresponding to the hyperbolic orbit at the cloudlet center. The periastron of the hyperbolic orbit, i.e., the centrifugal barrier, is set to be 50 au. Both the cloudlet and disk have an initial temperature of 78 K and a mean molecular weight of  $2.3 m_{\text{H}}$ .

We introduce the color (scalar) field,  $c$ , to trace the gas. It is assigned to be  $c = 1$  for the cloudlet,  $c = -1$  for the disk, and  $c = 0$  for the warm gas. We follow the change in the color by solving

$$\frac{\partial(c\rho)}{\partial t} + \nabla \cdot (c\rho \mathbf{v}) = 0, \quad (2.3)$$

simultaneously.

We denote the time,  $t$ , in yr and the distance in au. For further details, see Hanawa et al. (2022), on which this talk is based.

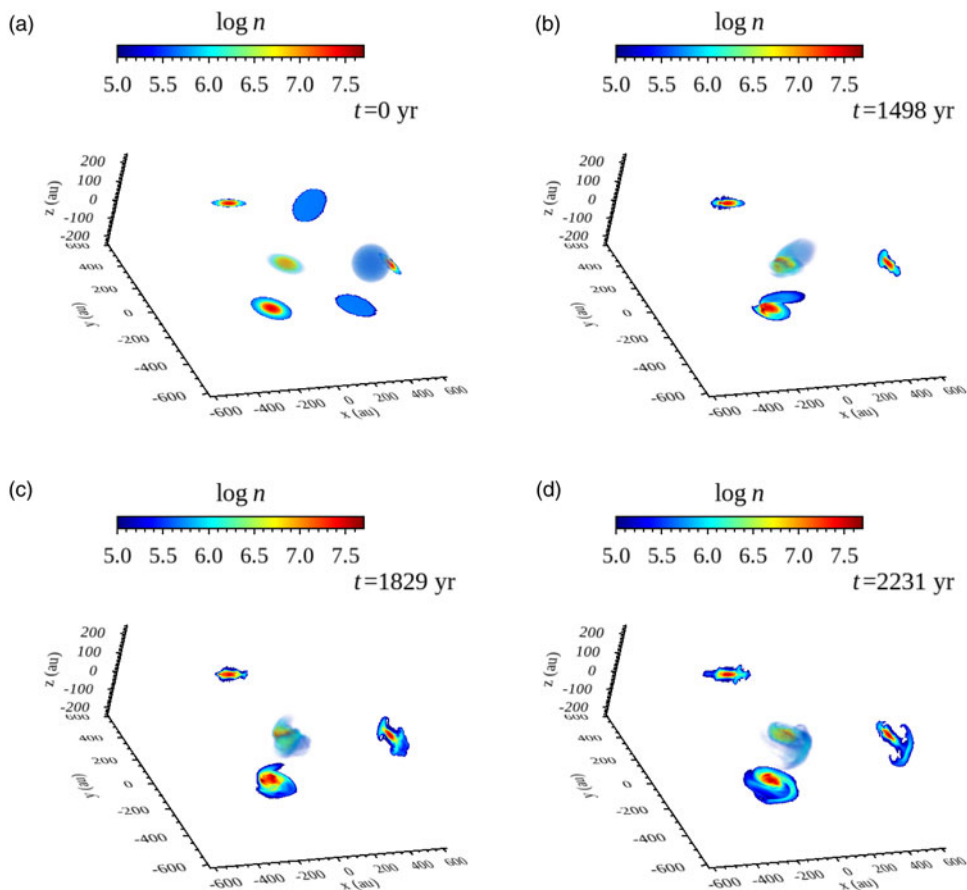


**Figure 1.** Evolution of the density distribution in model A in which the orbit of the cloudlet is coplanar to the rotating disk. Each panel shows the density by volume rendering in the center. The density distributions on the planes of  $x=0$ ,  $y=0$ , and  $z=0$  are projected on the right, deeper and lower sides, respectively.

### 3. Results

Figure 1 shows the density evolution in model A by a series of snapshots. Each panel displays the number density by volume rendering and cross sections. Note that our numerical model is scalable, i.e., still valid if both the density and pressure are magnified by an arbitrary factor. Thus, the color bar shows not the absolute density but a measure. Figure 1(a) shows the initial stage at  $t=0$ . The blue sphere on the right hand side denotes the cloudlet while the red disk surrounded by blue ring denotes the disk. The cloudlet is located at 500 au away from the central star and has the radius of 100 au. The disk radius is 100 au at the initial stage. At  $t=1498$  yr, the head of the cloudlet collides with the outer edge of the disk. The cloudlet rotates around the protostar while disturbing the pre-existing gas disk. The impact of the cloudlet forms spiral arms in the disk as shown in the cross sections of  $z=0$  in Figure 1 (c) and (d). Part of the cloudlet accretes onto the disk, whereas the rest leaves.

The cloudlet approaches the protostar from one side. Thus, it appears as a blue-shifted component to the left of the protostar if we observe it from the lefthand side in Figure 1, i.e., from the direction of  $x=-\infty$ . After the passage of the periastron, the cloudlet should appear as a red-shifted component to the right of the protostar. Hence, model A

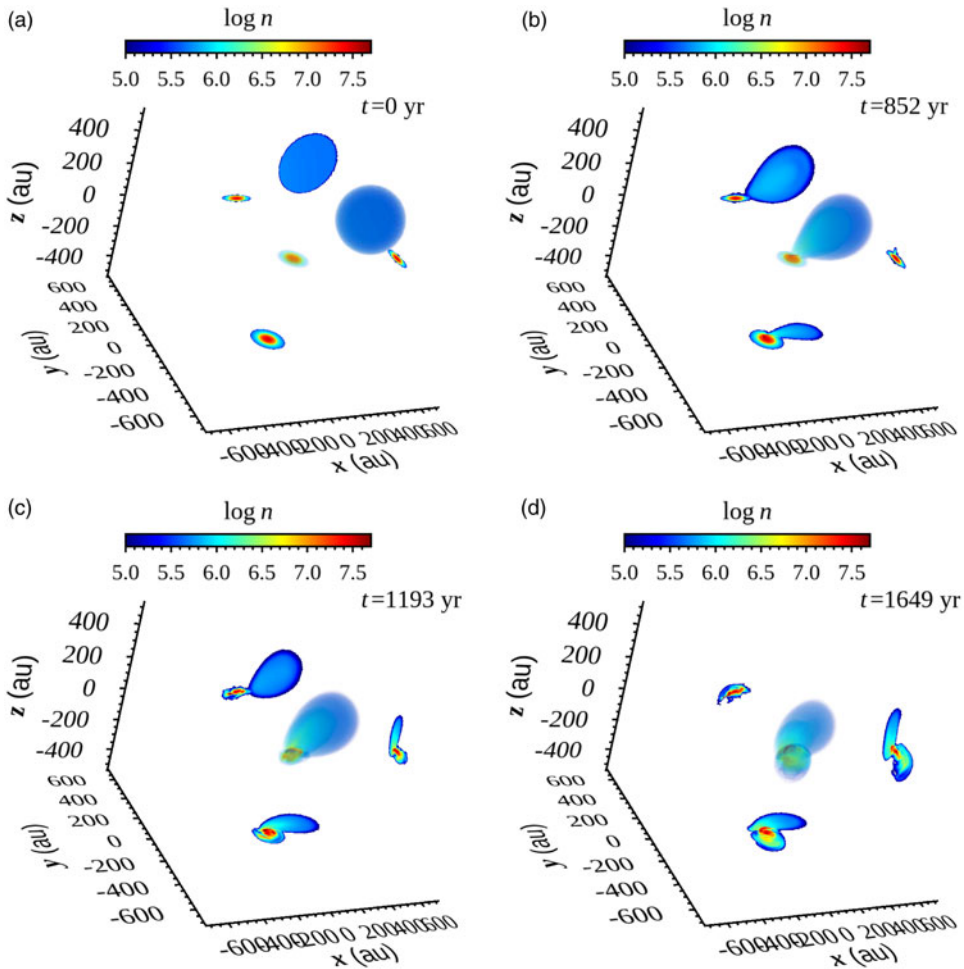


**Figure 2.** The same as Figure 1 but for model C.

can reproduce the blue asymmetry observed in TMC-1A qualitatively if we choose the appropriate stage.

Model A, however, mismatches the observations in some respects. First, the velocity of the infall is much higher than the observed one, about  $1.6 \text{ km s}^{-1}$ . The free-fall velocity reaches  $4.34 \text{ km s}^{-1}$  at the distance of 50 au from the star for the assumed stellar mass,  $0.53 M_{\odot}$ . Aso et al. (2015) suggested that the infall is decelerated by magnetic force from the observation of  $\text{C}^{18}\text{O}$  emission. Second, the cloudlet is too compact to explain the extension of the blue-shifted emission.

We have constructed model C to overcome the shortcomings mentioned. First, the orbital plane of the cloudlet is inclined to the disk plane so that they have different inclinations to the line of sight. If the orbital plane is nearly face-on, the line of sight velocity is much lower than the velocity in 3D. Thus far, the infall velocity has been derived under the assumption that the infalling gas shares the same orbital plane with the disk. The inclination is estimated from the oblateness of the disk shape measured from the radio continuum emission. The cloudlet is assumed to be spherical at the initial stage and to have the mass of  $1.02 \times 10^{-4} M_{\odot}$ . If such a cloudlet accretes onto the protostar every thousand years, the average mass accretion rate amounts to  $\dot{M} = 10^{-7} M_{\odot} \text{ yr}^{-1}$ .

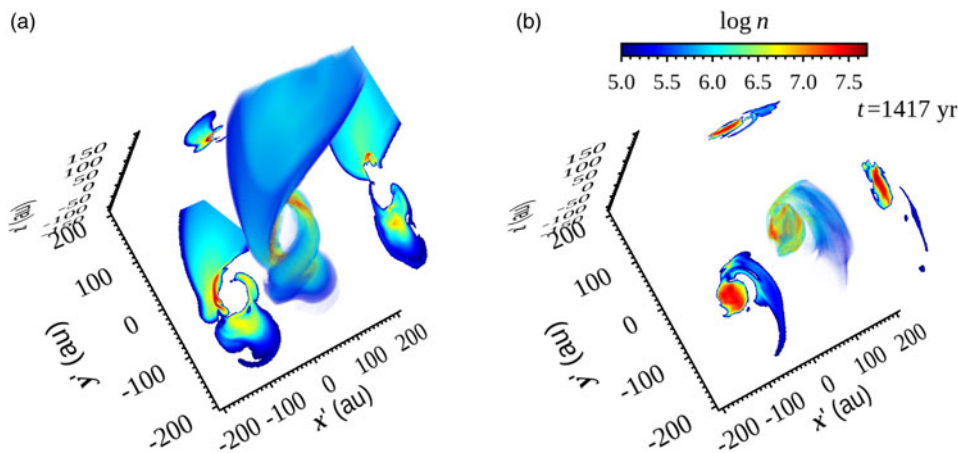


**Figure 3.** Each panel shows the cloudlet (a) and disk (b) at  $t = 1417$  yr in model E by the volume rendering and cross sections. The color scale is common.

Figure 2 is the same as Figure 1 but for model C. The orbital plane of the cloudlet is inclined by  $30^\circ$  to the disk plane in model C. The cloudlet has a radius of 200 au, and its center is located 500 au away from the protostar at the initial stage. The cloudlet reaches the gas disk earlier in model C than in model A [see Figure 2(b)]. As shown in Figure 2(c), the cloudlet hits the upper side of the disk to form spiral arms. The head of the cloudlet goes through the disk midplane at a later stage shown in Figure 2(d).

The cloudlet changes its shape and size while approaching the protostar. The tidal force of the protostar elongates the cloudlet in the direction of the orbit and the warm gas confines the cloudlet through the pressure. Though the elongation and confinement are seen in model A, they are more prominent in model C.

Our numerical model is similar to those of Dullemond et al. (2019) and Küffmeyer et al. (2020, 2021) except for the presence of the warm gas. The cloudlet expands to form an extended second-generation disk in their simulations, while it evolves into an elongated stream in our simulations. The difference is that the confinement of cloudlet is ascribed to the warm gas.

Figure 3 shows the cloudlet and disk at  $r = 1417$  yr separately. The viewing angles are different from that of Figure 2, and the horizontal coordinates are rotated by  $37.5^\circ$ ,

$$(x', y') = (x \cos 37.5^\circ + y \sin 37.5^\circ, -x \sin 37.5^\circ + y \cos 37.5^\circ). \quad (3.1)$$

A part of the cloudlet already passed the periastron, though the main part is still approaching the periastron. The former can be seen as a minor red-shifted component if we observe it in this viewing angle. Figure 3(a) shows that the collision of the cloudlet with the disk produces a shock wave. The shock compression should increase the temperature temporarily and changes its chemical composition accordingly.

The outer part of the disk is detached from the inner part to form a large spiral arm. The impact on the disk depends on the ratio of the cloudlet mass to the disk mass. Because the disk has the same mass in models A and C, the impact is larger in model C.

#### 4. Comparison with Observations

Our model C can reproduce several features observed in the molecular emission lines from TMC-1A. First, the model can explain the blue asymmetry observed in CS ( $J = 2 - 1$ ) line (Sakai et al. 2016) if the viewing angle is set appropriately. The cloudlet is chemically fresh, i.e., its chemical composition is close to that of a molecular cloud.

Second, it can resolve the issue of apparently slow infall estimated from the C<sup>18</sup>O line emission by Aso et al. (2015) under the assumption that the orbital plane is inclined to the disk plane and nearly faced on. Third, it can explain the asymmetry that the SO emission is offset to the south from the protostar. The impact of the cloudlet onto the disk induces a shock wave and releases SO from the dust through sputtering and shattering. To match the observation, the cloudlet should approach the protostar from the Northwest and the orbital plane should be close to the plane, though the Northwest side should be far from us.

A warm atomic gas is an important constituent in our model, though it is neither visible in our model nor in observations because of the low density. However, the warm gas confines the cloudlet by the pressure and assists its elongation. If the gas pressure is much lower, the cloudlet disperses to form an extended arc or a disk as shown by Dullemond et al. (2019) and Küffmeier et al. (2020, 2021). The shape of newly accreted molecular gas can serve as a probe of the environment around the young stellar objects.

This work was supported by JSPS KAKENHI Grant Nos. JP18H05222, JP19K03906, JP20H05845, JP20H05847, JP20H00182.

## References

- Aso, Y., Ohashi, N., Saigo, K. et al. 2015, *ApJ*, 812, 27  
Dullemond, C.P., Küffmeier, M., Goicovic, F. et al. 2019, *A&Ap*, 628, A20  
Garufi, A., Podio, L. Codella, C. et al. 2022, *A&Ap*, 658, A104.  
Hanawa, T., Matsumoto, Y. 2021, *ApJ*, 907, 43  
Hanawa, T., Sakai, N., Yamamoto, S. 2022, *ApJ*, 932, 122.  
Küffmeier, M., Goicovic, F.G., Dullemond, C.P. 2020, *A&Ap*, 633, 3  
Küffmeier, M., Dullemond, C.P., Reissi, S., Goicovic, F.G. 2020, *A&Ap*, 656, 161  
Sakai, N., Oya, Y., López Sepulcre, A. et al. 2016, *ApJ* (Letters), 820, L34  
Yen, H.-W., Takakuwa, S., Ohashi, N. et al. 2014, *ApJ*, 793, 1

## Discussion

BISIKALO: How high is the temperature of the cold gas?

HANAWA: The temperature of the cold gas is a little high and about 80 K.

BISIKALO: How did you take into account the viscosity?

HANAWA: The gas is assumed to be inviscid because it accretes onto the disk on a dynamic timescale. The viscosity has little effect on the accretion flow even if we take into account the viscosity of Shakura–Sunyaev type of  $\alpha \simeq 0.1$ .

BISIKALO: Did you take into account the self-gravity?

HANAWA: No.